Journal of Organometallic Chemistry 695 (2010) 841–849

Contents lists available at ScienceDirect

Journal of Organometallic Chemistry

journal homepage: www.elsevier.com/locate/jorganchem

Synthesis and characterization of complexes imparting *N*-pyridyl bonded *meso*-pyridyl substituted dipyrromethanes

Mahendra Yadav, Ashish Kumar Singh, Rampal Pandey, Daya Shankar Pandey *

Department of Chemistry, Faculty of Science, Banaras Hindu University, Varanasi 221 005, UP, India

ARTICLE INFO

Article history:
Received 6 November 2009
Received in revised form 29 December 2009
Accepted 4 January 2010
Available online 11 January 2010

Keywords:
Ruthenium
Rhodium
Iridium
Arene
Pentamethylcyclopentadienyl
Catalytic activity

ABSTRACT

The *meso*-pyridyl substituted dipyrromethane ligands 5-(4-pyridyl)dipyrromethane (4-dpmane) and 5-(3-pyridyl)dipyrromethane (3-dpmane) have been employed in the synthesis of a series of complexes with the general formulations $[(\eta^6\text{-arene})RuCl_2(L)]$ (η^6-arene = C_6H_6, $C_{10}H_{14}$) and $[(\eta^5\text{-}C_5Me_5)MCl_2(L)]$ (M = Rh, Ir). The reaction products have been characterized by microanalyses and spectral studies and molecular structures of the complexes $[(\eta^6\text{-}C_{10}H_{14})RuCl_2(4\text{-dpmane})]$ and $[(\eta^5\text{-}C_5Me_5)IrCl_2(3\text{-dpmane})]$ have been determined crystallographically. For comparative studies, geometrical optimization have been performed on the complex $[(\eta^5\text{-}C_5Me_5)IrCl_2(4\text{-dpmane})]$ using exchange correlation functional B3LYP. Optimized bond length and angles are in good agreement with the structural data of the complex $[(\eta^5\text{-}C_5Me_5)IrCl_2(3\text{-dpmane})]$. The complexes $[(\eta^6\text{-}C_{10}H_{14})RuCl_2(3\text{-dpmane})]$, $[(\eta^5\text{-}C_5Me_5)RhCl_2(3\text{-dpmane})]$ and $[(\eta^5\text{-}C_5Me_5)IrCl_2(3\text{-dpmane})]$ have been employed as a transfer hydrogenation catalyst in the reduction of aldehydes. It was observed that the rhodium and iridium complexes mentioned above are more effective in this regard in comparison to the ruthenium complex.

1. Introduction

Dipyrromethanes are important building blocks for many of the structures of interest in the areas of porphyrins, materials science, optics, and medicine [1–9]. A variety of conditions have been established for the synthesis of dipyrromethanes of diverse structures, from substituted pyrroles to unsubstituted pyrrole and carbonyl compounds [10]. The dipyrromethanes can be oxidatively converted to dipyrromethenes which are fully conjugated flat bipyrrolic moieties, and as such, are useful ligands for chelation to transition metals [11–14]. Although, numerous homo-/heteroleptic complexes based on dipyrrins are reported in the literature, use of dipyrromethanes as ligand has scarcely been reported [15–20]. Furthermore, there has been growing interest in the synthesis of complexes containing η^6-arene ruthenium, and η^5-C_5Me_5 rhodium/iridium complexes because of their catalytic potential and use as precursors in the synthesis of other Ru(II), Rh(III), and Ir(III) complexes [21–27]. In this regard dimeric arene ruthenium $[\{(\eta^6\text{-arene})Ru(\mu\text{-Cl})Cl\}_2]$ (arene = benzene and their derivatives) and structurally analogous rhodium and iridium complexes $[\{(\eta^5\text{-}C_5Me_5)M(\mu\text{-Cl})Cl\}_2]$ (M = Rh or Ir) have proved to be indispensable synthetic precursors [21–27]. Although, reactions of these dimers with a variety of Lewis bases, monodentate ligands, dipyrrins, chiral bidentate ligands, amino acids, peptides, and nucleobases have been studied extensively [28–40], their reactivity with *meso*-substituted dipyrromethanes have not been examined.

Recently, we have reported the synthesis, spectral, electrochemical and structural characterization of complexes based on η^6-arene ruthenium and η^5-C_5Me_5 rhodium/iridium moieties containing various dipyrrin ligands [37–40]. To develop coordination chemistry of dipyrromethane ligands we have examined reactivity of the dimers $[\{(\eta^6\text{-arene})Ru(\mu\text{-Cl})Cl\}_2]$ (arene = benzene and its derivatives), and $[\{(\eta^5\text{-}C_5Me_5)M(\mu\text{-Cl})Cl\}_2]$ with 5-(4-pyridyl)dipyrromethane (4-dpmane) and 5-(3-pyridyl)dipyrromethane (3-dpmane). In this article we report the synthesis and characterization of mononuclear pyridyl N-bonded ruthenium complexes $[(\eta^6\text{-arene})RuCl_2(L)]$ and rhodium/iridium complexes $[(\eta^5\text{-}C_5Me_5)MCl_2(L)]$ (M = Rh, Ir) and crystal structures of the complexes $[(\eta^5\text{-}C_{10}H_{14})RuCl_2(3\text{-dpmane})]$ and $[(\eta^5\text{-}C_5Me_5)IrCl_2(3\text{-dpmane})]$. Also, we describe herein our findings on geometrical optimizations performed on the complex $[(\eta^5\text{-}C_5Me_5)IrCl_2(4\text{-dpmane})]$ using exchange correlation functional B3LYP and application of the complexes $[(\eta^6\text{-}C_{10}H_{14})RuCl_2(3\text{-dpmane})]$, $[(\eta^5\text{-}C_5Me_5)RhCl_2(3\text{-dpmane})]$ and $[(\eta^5\text{-}C_5Me_5)IrCl_2(3\text{-dpmane})]$ in transfer hydrogenation catalysis of terephthaldehyde, 4-cyanobenzaldehyde and 4-nitrobenzaldehyde to corresponding alcohol.

2. Experimental

Analytical or chemically pure grade reagents were used throughout. All the reactions were carried out under nitrogen

* Corresponding author. Tel.: +91 542 6702480; fax: +91 542 2368174.
E-mail address: dspbhu@bhu.ac.in (D.S. Pandey).

0022-328X/$ - see front matter © 2010 Elsevier B.V. All rights reserved.
doi:10.1016/j.jorganchem.2010.01.006

atmosphere. The solvents were dried and distilled by standard procedures before use [41]. Hydrated ruthenium(III) chloride, hydrated rhodium(III) chloride, hydrated iridium(III) chloride, pentamethylcyclopentadiene, 1,3-cyclohexadiene, α-phellandrene (Aldrich) were used as received. The ligands 5-(4-pyridyl)dipyrromethane, 5-(3-pyridyl)dipyrromethane [42] and precursor complexes $[\{(\eta^6\text{-arene})Ru(\mu\text{-}Cl)Cl\}_2]$ (arene = benzene [43], *p*-cymene [44]), $[\{(\eta^5\text{-}C_5Me_5)Rh(\mu\text{-}Cl)Cl\}_2]$ [45], $[\{(\eta^5\text{-}C_5Me_5)Ir(\mu\text{-}Cl)Cl\}_2]$ [46] were prepared and purified following the literature procedures. Microanalyses were performed on a Exter CE-440 CHN Analyzer. IR and electronic absorption spectra were recorded on a Perkin–Elmer-577 and Shimadzu-UV 1700 spectrophotometers, respectively. ^1H and ^{13}C NMR spectra were acquired on a JEOL AL 300 FT-NMR machine in chloroform-*d* at 298 K using TMS as an internal reference. Emission spectra were recorded in dichloromethane on a Varian Cary Eclipse Fluorescence spectrophotometer at room temperature.

2.1. Syntheses

2.1.1. Preparation of $[(\eta^6\text{-}C_6H_6)RuCl_2(4\text{-dpmane})]$ (1)

To a suspension of $[\{(\eta^6\text{-}C_6H_6)Ru(\mu\text{-}Cl)Cl\}_2]$ (125 mg, 0.250 mmol) in dichloromethane (25 mL), 5-(4-pyridyl)dipyrromethane (112 mg, 0.500 mmol) was added and stirred at room temperature for 4 h. It gave a clear pale red solution which was filtered through Celite to remove any solid impurities. Addition of hexane to the filtrate afforded pale red crystalline product. It was separated by filtration washed with diethyl ether and dried under *vacuum*. Yield: 180 mg, 76%, m.p. 135 °C (decomp.). Microanalytical data: $C_{20}H_{19}N_3Cl_2Ru$, requires: C, 50.75; H, 4.05; N, 8.88. Found: C, 51.04; H, 4.20; N, 8.80%. IR (KBr pellets, cm^{-1}): 3345, 3065, 2925, 1610, 1550, 1429, 1093, 806, 673, 473. ^1H NMR ($CDCl_3$, δ ppm): 8.76 (d, 2H, J = 6.0 Hz), 8.15 (bs, 2H), 7.02 (d, 2H, J = 6.0 Hz), 6.67(d, 2H, J = 0.9 Hz), 6.10 (dd, 2H, J = 3.0, 2.4 Hz), 5.77 (bs, 2H), 5.63 (s, 6H), 5.46 (s, 1H). UV–Vis {CH_2Cl_2, λ nm (ε)}: 413 (2.20×10^3), 290 (1.17×10^4), 242 (2.10×10^4).

2.1.2. Preparation of $[(\eta^6\text{-}C_6H_6)RuCl_2(3\text{-dpmane})]$ (2)

Complex **2** was prepared from $[\{(\eta^6\text{-}C_6H_6)Ru(\mu\text{-}Cl)Cl\}_2]$ (125 mg, 0.250 mmol) and 5-(3-pyridyl)dipyrromethane (112 mg, 0.500 mmol) following the method employed for **1**. Yield: 177 mg, 75%, m.p. 139 °C (decomp.). Microanalytical data: $C_{20}H_{19}N_3Cl_2Ru$, requires: C, 50.75; H, 4.05; N, 8.88. Found: C, 51.04; H, 4.18; N, 8.80%. IR (KBr pellets, cm^{-1}): 3349, 3050, 1610, 1560, 1472, 1429, 1040, 1035, 823, 734, 584. ^1H NMR ($CDCl_3$, δ ppm): 9.04 (s, 1H), 8.94 (d, 1H, J = 5.1 Hz), 8.27 (bs, 2H), 7.56 (m, 1H), 7.26 (m, 1H), 6.73 (bs, 2H), 6.15 (bs, 2H), 5.86 (bs, 2H), 5.62 (s, 6H), 5.48 (s, 1H). UV–Vis {CH_2Cl_2, λ nm (ε)}: 411 (2.24×10^3), 273 (1.11×10^4), 239 (1.98×10^4).

2.1.3. Preparation of $[(\eta^6\text{-}C_{10}H_{14})RuCl_2(4\text{-dpmane})]$ (3)

This complex was prepared using $[\{(\eta^6\text{-}C_{10}H_{14})Ru(\mu\text{-}Cl)\ Cl\}_2]$ (153 mg, 0.250 mmol) and 5-(4-pyridyl)dipyrromethane (112 mg, 0.500 mmol) following the method for **1**. Yield: 212 mg, 80%, m.p. 137 °C (decomp.). Microanalytical data: $C_{24}H_{27}N_3Cl_2Ru$, requires: C, 54.44; H, 5.14; N, 7.94. Found: C, 54.68; H, 5.29; N, 7.83%. IR (KBr pellets, cm^{-1}): 3326, 3099, 2962, 1612, 1561, 1465, 1427, 1040, 1030, 901, 774, 728, 620, 528. ^1H NMR ($CDCl_3$, δ ppm): 8.66 (d, 2H, J = 6.0 Hz), 8.28 (bs, 2H), 6.95 (d, 2H, J = 6.0 Hz), 6.62 (bs, 2H), 6.07 (d, 2H, J = 2.1 Hz), 5.77 (bs, 2H), 5.43 (d, 3H, J = 5.7 Hz), 5.21 (d, 2H, 5.7 Hz), 2.98 (m, 1H), 2.06 (s, 3H), 1.30 (d, 6H, J = 6.9). UV–Vis {CH_2Cl_2, λ nm (ε)}: 416 (2.2×10^3), 294 (1.15×10^4), 239 (2.30×10^4).

2.1.4. Preparation of $[(\eta^6\text{-}C_{10}H_{14})RuCl_2(3\text{-dpmane})]$ (4)

This complex was prepared using $[\{(\eta^6\text{-}C_{10}H_{14})Ru(\mu\text{-}Cl)\ Cl\}_2]$ (153 mg, 0.250 mmol) and 5-(3-pyridyl)dipyrromethane (112 mg, 0.500 mmol) following the above procedure for **1**.Yield: 201 mg, 76%, m.p. 135 °C (decomp.). Microanalytical data: $C_{24}H_{27}N_3Cl_2Ru$, requires: C, 54.44; H, 5.14; N, 7.94. Found: C, 54.75; H, 5.26; N, 7.83%. IR (KBr pellets, cm^{-1}): 3340, 3047, 1610, 1564, 1470, 1425, 1032, 1028, 971, 779, 734, 584. ^1H NMR ($CDCl_3$, δ ppm): 8.92 (s, 1H), 8.86 (d, 1H, J = 5.4 Hz), 8.34 (bs, 2H), 7.53 (m, 1H), 7.20 (m, 1H), 6.71 (bs, 2H), 6.13 (d, 2H, J = 2.1 Hz), 5.85 (bs, 2H), 5.47 (s, 1H), 5.39 (d, 2H, 5.7 Hz), 5.17 (d, 2H, J = 6.0 Hz), 2.89 (m, 1H), 2.02 (s, 3H), 1.25 (d, 6H, J = 7.2 Hz). UV–Vis {CH_2Cl_2, λ nm (ε)}: 418 (2.86×10^3), 288 (1.15×10^4), 239 (2.32×10^4).

2.1.5. Preparation of $[(\eta^5\text{-}C_5Me_5)RhCl_2(4\text{-dpmane})]$ (5)

It was prepared from $[\{(\eta^5\text{-}C_5Me_5)Rh(\mu\text{-}Cl)\ Cl\}_2]$ (154 mg, 0.250 mmol) and 5-(4-pyridyl)dipyrromethane (112 mg, 0.500 mmol) following the above procedure for **1**. Yield: 207 mg, 78%, m.p. 146 °C (decomp.). Microanalytical data: $C_{24}H_{28}N_3Cl_2Rh$, requires: C, 54.15; H, 5.30; N, 7.89. Found: C, 54.42; H, 5.42; N, 7.82%. IR (KBr pellets, cm^{-1}): 3340, 2923, 2857, 1613, 1558, 1460, 1426, 1377, 1093, 1026, 728, 673, 598, 522. ^1H NMR ($CDCl_3$, δ ppm): 8.63 (d, 2H, J = 5.1 Hz), 8.40 (bs, 2H), 7.05 (d, 2H, J = 5.4 Hz), 6.66 (bs, 2H), 6.05 (bs, 2H), 5.71 (bs, 2H), 5.51 (s, 1H), 1.60 (s, 15H). UV–Vis {CH_2Cl_2, λ nm (ε)}: 402 (3.2×10^3), 268 (9.97×10^3), 238 (2.25×10^4).

2.1.6. Preparation of $[(\eta^5\text{-}C_5Me_5)RhCl_2(3\text{-dpmane})]$ (6)

Complex **6** was prepared from $[\{(\eta^5\text{-}C_5Me_5)Rh(\mu\text{-}Cl)Cl\}_2]$ (154 mg, 0.250 mmol) and 5-(3-pyridyl)dipyrromethane (112 mg, 0.500 mmol) following the procedure employed for **1**. Yield: 202 mg, 80%, m.p. 145 °C (decomp.). Microanalytical data: $C_{24}H_{28}N_3Cl_2Rh$, requires: C, 54.15; H, 5.30; N, 7.89. Found: C, 54.39; H, 5.45; N, 7.80%. IR (KBr pellets, cm^{-1}): 3352, 2925, 1613, 1567, 1468, 1426, 1117, 1032, 730, 588. ^1H NMR ($CDCl_3$, δ ppm): 8.83 (d, 1H, J = 4.5 Hz), 8.80 (s, 1H), 8.25 (bs, 2H), 7.55 (m, 1H), 7.26 (m, 1H), 6.73 (bs, 2H), 6.14 (d, 2H, J = 3.0 Hz), 5.85 (bs, 2H), 5.50 (s, 1H), 1.60 (s, 15H). UV–Vis {CH_2Cl_2, λ nm (ε)}: 401 (2.74×10^3), 268 (1.17×10^4), 239 (2.06×10^4).

2.1.7. Preparation of $[(\eta^5\text{-}C_5Me_5)IrCl_2(4\text{-dpmane})]$ (7)

This complex was prepared using $[\{(\eta^5\text{-}C_5Me_5)Ir(\mu\text{-}Cl)Cl\}_2]$ (199 mg, 0.250 mmol) and 5-(4-pyridyl)dipyrromethane (112 mg, 0.500 mmol) following the above procedure for **1**. Yield: 233 mg, 75%, m.p. 177 °C (decomp.). Microanalytical data: $C_{24}H_{28}N_3Cl_2Ir$, requires: C, 46.37; H, 4.54; N, 6.76. Found: C, 46.67; H, 4.70; N, 6.67%. IR (KBr pellets, cm^{-1}): 3342, 2925, 1612, 1558, 1463, 1428, 1370, 1093, 1026, 729, 598. ^1H NMR ($CDCl_3$, δ ppm): 8.75(d, 2H, J = 6.0 Hz), 8.17 (bs, 2H), 7.11(d, 2H, J = 5.7 Hz), 6.71 (bs, 2H), 6.12 (d, 2H, J = 2.1 Hz), 5.79 (bs, 2H), 5.54 (s, 1H), 1.56 (s, 15H). UV–Vis {CH_2Cl_2, λ nm (ε)}: 445 (1.57×10^3), 280 (1.16×10^4), 238 (2.32×10^4).

2.1.8. Preparation of $[(\eta^5\text{-}C_5Me_5)IrCl_2(3\text{-dpmane})]$ (8)

It was prepared from $[\{(\eta^5\text{-}C_5Me_5)Ir(\mu\text{-}Cl)Cl\}_2]$ (199 mg, 0.250 mmol) and 5-(3-pyridyl)dipyrromethane (112 mg, 0.500 mmol) following the above procedure for **1**. Yield: 230 mg, 74%, m.p. 175 °C (decomp.). Microanalytical data: $C_{24}H_{28}N_3Cl_2Ir$, requires: C, 46.37; H, 4.54; N, 6.76. Found: C, 46.69; H, 4.68; N, 6.70%. IR (KBr pellets, cm^{-1}): 3350, 2923, 1615, 1570, 1464, 1427, 1110, 1030, 729, 585. ^1H NMR ($CDCl_3$, δ ppm): 8.86 (d, 1H, J = 4.8 Hz), 8.80 (s, 1H), 8.28 (bs, 2H), 7.57 (m, 1H), 7.26 (m, 1H), 6.74 (bs, 2H), 6.14 (d, 2H, J = 3.0 Hz), 5.86 (bs, 2H), 5.52 (s, 1H), 1.56 (s, 15H). UV–Vis {CH_2Cl_2, λ nm (ε)}: 435 (9.27×10^2), 276 (1.16×10^4), 240 (2.06×10^4).

2.2. X-ray crystallography

2.2.1. Details of single crystal X-ray diffraction study

A detail about the data collection, solution and refinement is summarized in Section 2.2.2. Intensity data for **3** and **8** were collected on a OXFORD DIFFRACTION X CALIBUR-S diffractometer equipped with graphite Mo-Kα radiation ($\lambda = 0.71073$ Å) at 293(2) K. The structures were solved by direct methods (SHELXS 97) and refined by full-matrix least squares procedure based on F^2 (SHELX 97) [47]. All the non-hydrogen atoms were refined anisotropically and hydrogen atoms were located at calculated positions and refined using a riding model with isotropic thermal parameters fixed at 1.2 times the U_{eq} value of the appropriate carrier atom.

2.2.2. Selected crystallographic data

2.2.2.1. Complex ***3***. Formula = $C_{24}H_{27}Cl_2N_3Ru$, Mw = 529.46, specimen 0.28 mm × 0.23 mm × 0.19 mm, monoclinic space group *P21/c*, $a = 14.3658(3)$, $b = 9.70120(10)$, $c = 17.3090(3)$ Å; $\beta = 106.787(2)°$; $V = 2309.48(7)$ Å^3; $Z = 4$; D_{calc} 1.523 g cm^{-3}, $F(0\,0\,0) = 1080$, $\mu = 0.926$, $T(K) = 150(2)$, $\lambda = 0.71073$, R(all) = 0.0237, $R(I > 2\sigma\ (I)) = 0.0198$, $wR2 = 0.0504$, $wR2\ [I > 2\sigma\ (I)] = 0.0494$, GOF = 1.043.

2.2.2.2. Complex ***8***. Formula = $C_{24.50}H_{26}Cl_3N_3Ir$, Mw = 661.03, specimen 0.15 mm × 0.13 mm × 0.12 mm, monoclinic space group *C2/c*, $a = 22.180(2)$, $b = 10.2552(12)$, $c = 21.9926(18)$ Å; $\beta = 101.374(9)$, $V = 4904.2(9)$ Å^3; D_{calc} 1.791 g cm^{-3}, $F(0\,0\,0) = 2576$, $\mu = 5.790$, $T(K) = 150(2)$, $\lambda = 0.71073$, R(all) = 0.0786, $R(I > 2\sigma\ (I)) = 0.0595$, $wR2 = 0.1613$, $wR2\ [I > 2\sigma\ (I)] = 0.1509$, GOF = 1.080.

2.3. Computational methods

Calculations were performed using hybrid B3LYP density functional method which uses Becke's 3-parameter non-local exchange functionals mixed with exact (Hartree–Fock) exchange functional and Lee–Yang–Parr's non-local correlation functional [48,49]. Geometries of the complex **7** was optimized without any symmetry restrictions with standard 6-31G** basis sets [50,51] for N, C, H and Cl and LANL2DZ [52–54] for Ir, which combines quasi-relativistic effective core potentials with a valence double-basis set. Electronic structure of the complex was examined by natural charges at each atom computed using Kohn-Sham orbitals obtained from DFT calculations [55]. The calculations were performed using GAUSSIAN 03 program [56].

3. Results and discussion

3.1. Syntheses and characterization

The dipyrromethane ligands were synthesized by reaction of 4-/3-pyridyl carboxaldehyde and an excess of pyrrole following the literature procedures [42]. Recently we have employed these ligands in the synthesis of dipyrrin complexes and have used the resulting dipyrrin complexes as a synthon in the synthesis of homo-/hetero-binuclear complexes containing η^6-arene ruthenium and η^5-C_5Me_5 rhodium/iridium moieties [40]. In the present work reactions of the dipyrromethane ligands have directly been investigated with the chloro-bridged dimers $[\{(\eta^6\text{-arene})Ru(\mu\text{-}Cl)Cl\}_2]$ (η^6-arene = benzene, *p*-cymene) and $[\{(\eta^5\text{-}C_5Me_5)M(\mu\text{-}Cl)Cl\}_2]$ (M = Rh, Ir).

Reactions of the chloro-bridged dimeric complexes $[\{(\eta^6\text{-arene})Ru(\mu\text{-}Cl)Cl\}_2]$ with 4-/3-dpmane in dichloromethane in 1:2 molar ratio gave mononuclear complexes with the general formulations $[(\eta^6\text{-arene})RuCl_2(L)]$ (η^6-arene = benzene, L = 4-dpmane **1**; η^6-arene = benzene, L = 3-dpmane **2**; η^6-arene = *p*-cymene, L = 4-dpmane **3**; η^6-arene = *p*-cymene, L = 3-dpmane **4**). Structurally analogous dimeric complexes $[\{(\eta^5\text{-}C_5Me_5)M(\mu\text{-}Cl)Cl\}_2]$ (M = Rh, Ir) reacted with these ligands under analogous conditions to afford the complexes $[(\eta^5\text{-}C_5Me_5)MCl_2(L)]$ **5**–**8** (M = Rh, L = 4-dpmane **5**; M = Rh, L = 3-dpmane **6**; M = Ir, L = 4-dpmane **7**; M = Ir, L = 3-dpmane **8**). A simple scheme depicting syntheses of **1**-**8** and is shown in Schemes 1 and 2. All the complexes have been isolated in reasonably good yields. These are air-stable, non-hygroscopic, golden-yellow crystalline solids, soluble in common organic solvents like acetone, dichloromethane, chloroform, dimethylformamide, dimethylsulfoxide, methanol, and ethanol and insoluble in diethyl ether petroleum ether and hexane. The complexes under investigation have been characterized by elemental analyses, spectral (IR, NMR electronic and emission) studies and molecular structures of **3** and **8** have been authenticated crystallographically.

The complexes **1**–**8** have analogous coordination environment about the respective metal centres (ruthenium, rhodium or iridium), and displayed an analogous pattern of resonances in its ^{1}H NMR spectra. In general, pyridyl protons (a, b protons of 4-dpmane and a, b, c, d protons of 3-dpmane Fig. S1) of the respective ligands exhibited a downfield shift in comparison to the uncoordinated ligand [42], while other protons (pyrrolic and *meso*-) did not show any appreciable shift. For example, in the ^{1}H NMR spectrum of **1**, protons associated with η^6-C_6H_6 resonated as a singlet at $\delta \sim 5.63$ (s, 6H) ppm and ligand protons at ~8.76 (d, 2H, 2,6-Py),

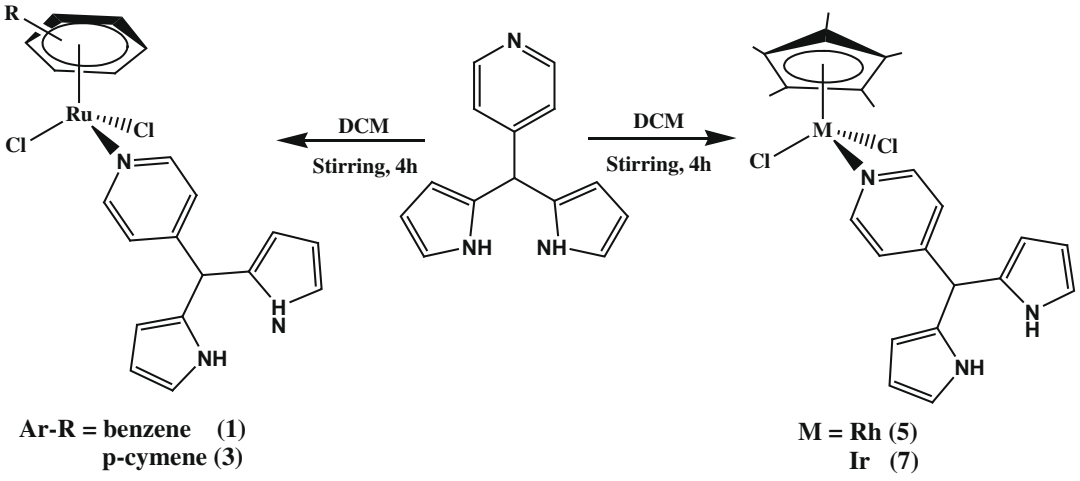

Ar-R = benzene (1)
p-cymene (3)

M = Rh (5)
Ir (7)

Scheme 1. Synthesis of complexes 1,3,5,7.

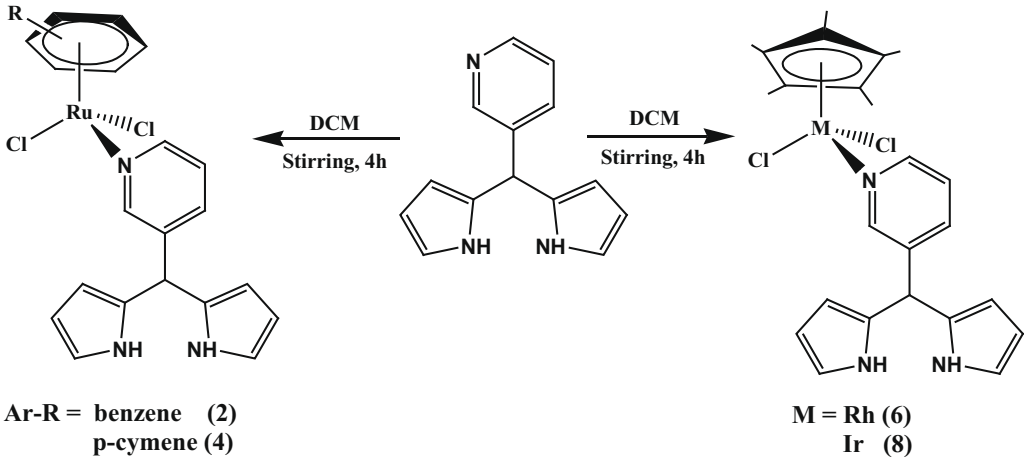

Scheme 2. Synthesis of complexes 2,4,6,8.

8.15 (bs, 2H, *N*-pyrrole), 7.02 (d, 2H, 3,5-Py), 6.67 (d, 2H, pyrrole), 6.10 (dd, 2H, pyrrole), 5.77 (bs, 2H, pyrrole), 5.46 (s, 1H, *meso*-H) ppm. It is observed that the arene protons in these complexes resonated at almost the same position as in the respective precursor complexes [43–46]. Further, the position of various peaks and integrated intensity under each peak strongly supported formation of the complexes and their proposed formulations.

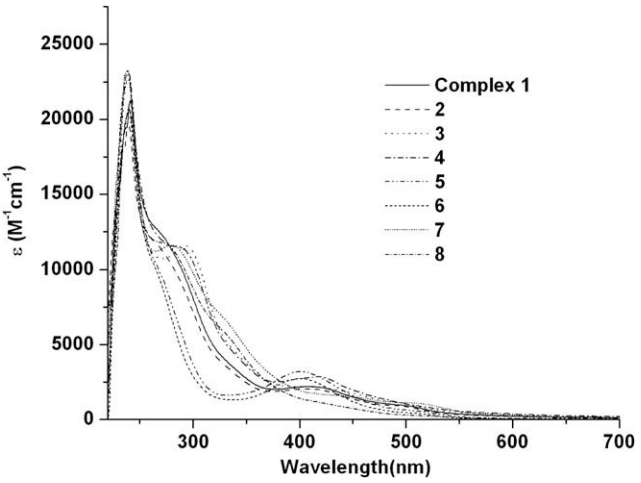

Fig. 1. Electronic absorption spectra of the complexes **1**–**8** in dichloromethane.

The electronic absorption spectra of **1–8** were acquired in dichloromethane at room temperature and resulting data is summarized in Section 2. The low spin d^6 orbitals on ruthenium(II)/rhodium(III)/iridium(III) provides filled t_{2g} orbitals of proper symmetry for interaction with relatively low lying unoccupied π^* orbitals of the ligand. It is expected to give a band associated with metal to ligand charge transfer transition (MLCT) ($t_2g \rightarrow \pi^*$) whose position varies with the nature of metal ion and ligands acting as π acceptor. The electronic spectra of **1**–**8** displayed bands at, ~413/411(**1**/**2**), ~416/418 (**3**/**4**) in ruthenium complexes and ~402/401(**5**/**6**), ~445/435(**7**/**8**) nm in the rhodium and iridium complexes, respectively. On the basis of its position and intensity it has been assigned as MLCT transitions [57–62] (Fig. 1). The bands at ~294 and 239 nm has been ascribed to the intra-ligand transitions ($n \rightarrow \pi^*/\pi \rightarrow \pi^*$). Presence of MLCT bands in the electronic absorption spectra of respective complexes support formation of the complexes. Emission spectra of **1–8** were acquired in dichloromethane at room temperature. Upon excitation at their respective MLCT bands, complexes did not show any appreciable emissions.

3.2. Molecular structure

Molecular structures of **3** and **8** have been determined crystallographically. Details about the data collection, solution and refinement is summarized in the crystallographic section, selected geometrical parameters are summarized in Table 1 and ORTEP views at 30% thermal ellipsoid probability is depicted in Figs. 2

Table 1
Selected bond length and angles for complexes **3** and **8**.

Bonds (Å)	**3**	**8**	Angle (°)	**3**	**8**
Ru1/Ir1–N1	2.1302(16)	2.110(7)	N1–Ru1/Ir1–Cl1	86.52(4)	89.4(2)
Ru1/Ir1–Cl1	2.4110(5)	2.128(9)	N1–Ru1/Ir1–Cl2	86.72(4)	84.8(2)
Ru1/Ir1–Cl2	2.4118(5)	2.135(9)	Cl1–Ru1/Ir1–Cl2	88.120(17)	88.59(9)
Ru1/Ir1–C_{ct}	1.659	1.761	Cl1–Ru1/Ir1–C_{ct}	128.10	125.80
Ru1/Ir1–C_{av}	2.181	2.146	Cl2–Ru1/Ir1–C_{ct}	126. 01	120.32
C13/14–C16	1.528(3)	1.520(13)	N1–Ru1/Ir1–C_{ct}	127.71	125.66
C16–C21	1.512(3)	1.478(13)	C13/14–C16–H16	106.5	106.6
C16–C17	1.509(3)	1.494(13)	C13/14–C16–C17	110.74(15)	109.8(8)
C16–H16	1.0000	1.0000	C13/14–C16–C21	113.22(16)	113.2(7)
N2–H2	0.8800	0.8800	C21–C16–C17	112.89(16)	113.5(9)
N3–H2	0.8800	0.8800			
C13/14–C16–C17–N3		−104.0(2)	61.8(11)		
C13/14–C16–C21–N2		135.10(19)	−129.5(10)		
C21–C16–C17–N3		127.83(19)	−170.4(8)		
C17–C16–C21–N2		−98.1(2)	104.5(11)		

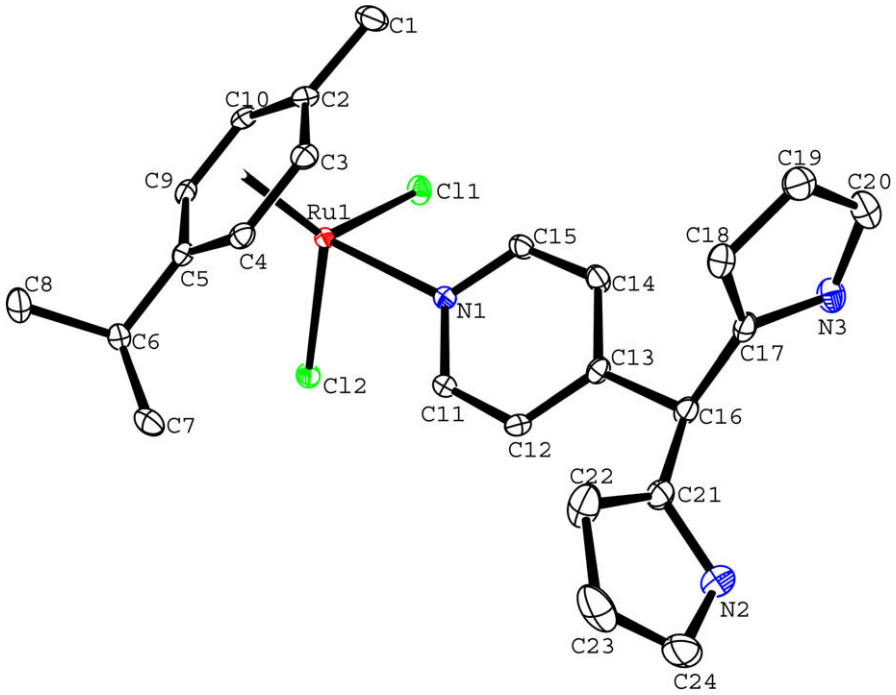

Fig. 2. ORTEP diagram of **3** at 30% thermal ellipsoid probability (H-atoms omitted for clarity).

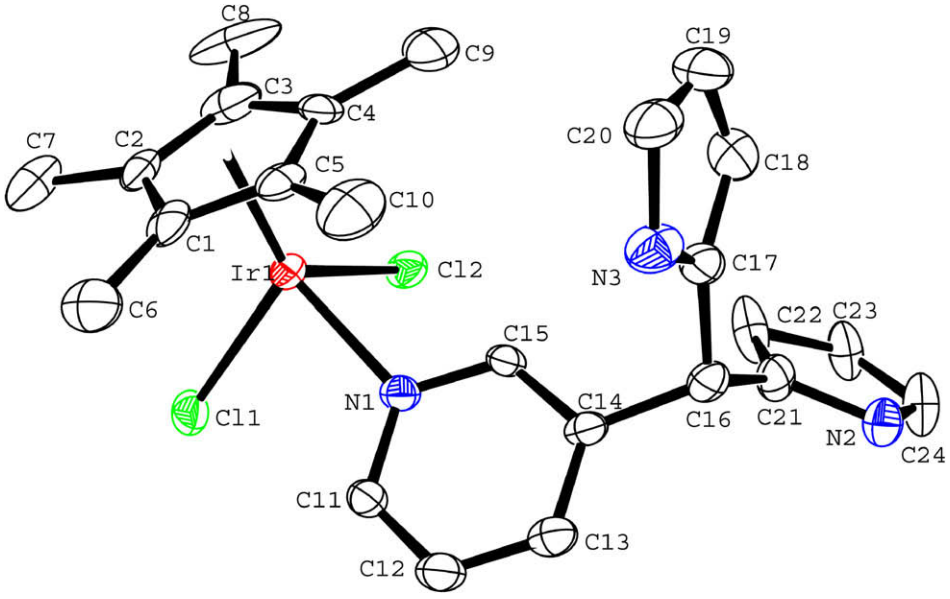

Fig. 3. ORTEP diagram of **8** at 30% thermal ellipsoid probability (H-atoms omitted for clarity).

and 3. Overall arrangement of the various ligands about metal centres ruthenium and iridium in **3** and **8** are analogous and the coordination geometry is typical "*piano-stool*" geometry. It is completed by pyridyl nitrogen of 4-dpmane, chloro- groups and *p*-cymene ring coordinated in η^6-manner in **3**, while in **8**, it is completed by pyridyl nitrogen from 3-dpmane, two chloro- groups and C_5Me_5 ring coordinated in η^5-manner. The M–N and M–Cl (M = Ru, Ir) bond distances [Ru–N1 = 2.130 Å, Ru–Cl1 = 2.411 Å, Ru–Cl2 = 2.412 Å in **3** and Ir–N1 = 2.110Å, Ir–Cl1 = 2.128Å, Ir–Cl2 = 2.135 Å in **8**] are normal [37,38]. The Cl–M–Cl and N–M–Cl angles are less than 90° [Cl1–Ru–Cl2 = 88.12°, N1–Ru–Cl1 = 86.52°, N1–Ru–Cl2 = 86.72° in **3** and Cl1–Ir–Cl2 = 88.59°, N1–Ir–Cl1 = 89.4°, N1–Ir–Cl2 = 84.8° in **8**] are consistent with the "*piano stool*" arrangement of various groups about the metal centres [Table 1] [57–62]. The M–C distances are almost equal with an average Ru–C = 2.181 [range 2.158–2.200 Å] and Ir–C = 2.146 Å [range 2.128–2.165 Å]. The metal to centroid of η^6-$C_{10}H_{14}$ ring and η^5-C_5Me_5 ring separations are 1.659, 1.761 Å, respectively and are close to those reported for other (η^6-$C_{10}H_{14}$)-Ru(II), (η^5-C_5Me_5)-Ir(III) complexes [37,38,62].

The X-ray crystal structures of the complexes exhibited that free pyrrolic N–H in these complexes are involved in strong hydrogen bonding interactions leading to a dimer in complex **3**, while a zig-zag structural motif along crystallographic-'a' axis in complex **8** (Figs. 4 and 5). In addition, weak interaction studies revealed the presence of various C–H···Cl, C–H···π, π···π interactions in the so-

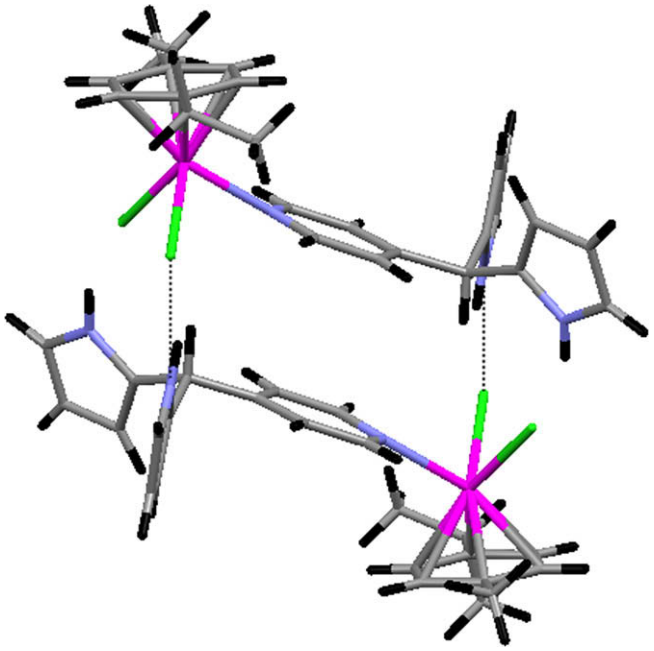

Fig. 4. Hydrogen bonding interaction leading to a dimeric structure in complex **3**.

lid state (Table 2). Contact distances between C–H···Cl, C–H···π, π···π are 2.71–2.84, 2.58–2.83 and 3.83–3.84 Å, respectively. These interactions may be called vdw interactions, since the lengths are significantly less than the sum of the van der Waals radii (2.8 and 3.1 Å, respectively). The C–H···Cl, C–H···π and π···π interactions in complexes resulted in a sheet like (Fig. 6 and S2) zig-zag motif (Fig. 7).

Table 2
Matrices for weak interactions for **3** and **8**.

X–H–Cg	H–Cg (Å)	H-(ring plane) (Å)	C–Cg (Å)	C–H–Cg (°)	γ (°)
Complex ***3***					
C(14)–H(14)···Cg(N3–C17–C18–C19–20)[a]	2.87	2.531	3.470(2)	122	28.14
C(18)–H(18)···Cg(N1–C11–C12–C13–C14–C15)[b]	2.90	2.830	3.632(2)	134	12.96
Complex ***8***					
N(3)–H(3)···Cg(N2–C21–C22–C23–C24)[c]	2.58	2.462	3.6853	162	17.14
C(10)–H(10B)···Cg(N3–C17–C18–C19–C20)[d]	2.85	2.593	3.748(16)	153	24.59

a = *X*, *Y*, *Z*; *b* = −*X*, 1 − *Y*, −*Z*; *c* = 1/2 − *X*, 1/2 + *Y*, 1/2 − *Z*; *d* = *X*, *Y*, *Z*

Complex ***8***	Cg–Cg	α (°)	β (°)	γ (°)
Cg(N3–C17–C18–C19–C20)–Cg(N1–C11–C12–C13–C14–C15)[a]	3.834(7)	24.57	21.97	28.08
Cg(C1–C2–C3–C4–C5)–Cg(C1–C2–C3–C4–C5)[b]	3.845(7)	0.00	16.55	16.55
Cg(N1–C11–C12–C13–C14–C15)–Cg(N3–C17–C18–C19–C20)[c]	3.834(7)	24.57	28.08	21.97

a = 1/2 − *X*, 1/2 + *Y*, 1/2 − *Z*; *b* = −*X*, 1 − *Y*, −*Z*; *c* = 1/2 − *X*, −1/2 + *Y*, 1/2 − *Z*

D–H···A	*D*(D–H)	*d*(H···A)	*d*(D···A	*L*(DHA)
Complex ***3*** *(Å and °)*				
N(2)–H(2)···Cl(1)[a]	0.88	2.49	3.304(2)	154
N(3)–H(3)···Cl(2)[a]	0.88	2.46	3.2155(18)	145
C(11)–H(11)···Cl(2)[a]	0.95	2.73	3.242(2)	114
C(16)–H(16)···Cl(1)[a]	1.00	2.71	3.575(2)	145
Complex ***8*** *(Å and °)*				
N(2)–H(2)···Cl(1)[b]	0.88	2.53	3.219(9)	136
C(10)–H(10B)···N(3)[b]	0.98	2.61	3.408(17)	139
C(11)–H(11)···Cl(1)[b]	0.95	2.74	3.286(10)	117
C(22)–H(22)···Cl(22)[b]	0.95	2.82	3.49(2)	128

a = −*x*, 2 − *y*, −*z*; *b* = 1/2 − *x*, 1/2 + *y*, 1/2 − *z*

3.3. Theoretical calculations

To establish the structure and verify geometrical parameters (bond length and bond angles) geometrical optimizations were performed on the complex **7**. Optimized geometry of the complex is shown in Fig. 8. One can see that the optimized bond lengths and bond angles for **7** are in good agreement with those obtained from X-ray diffraction analyses of structurally analogous complex **8** (Table S1). In addition, frequency calculations have been performed to check whether optimized geometries are minima on the potential energy surface or not.

We begin analysis of the bonding situation with a discussion of natural atomic charges. Natural bond orbital (NBO) charge distributions are presented in Scheme 3. To examine charge flow between the 4-dpmane and the [(η5-C_5Me_5)$IrCl_2$] metal fragments, we calculated atomic charges of the fragment in the frozen geometries of the molecules. The results are shown in Scheme 3(b). Scheme 3(c) shows that the Wiberg bond indices (WBI) of the Ir–N and Ir–Cl bonds are 0.37, 0.45 and 0.46, respectively. It suggested that in this complex the Ir–N/Cl bonds would be significantly more polar with a bond order less than one.

The calculated natural charge distribution indicated that the iridium atom, pentamethylcyclopentadienyl and 4-dpmane groups carry a significant positive charge, while the chloro ligands are negatively charged. Scheme 3(b) shows, that the η5-C_5Me_5 group in complex has a lower positive charge than those in the metal fragment [(η5-C_5Me_5)$IrCl_2$]. It is observed that there is net flow of charge in the direction from 4-dpmane to [(η5-C_5Me_5)$IrCl_2$]. The change in the charges of [(η5-C_5Me_5)$IrCl_2$] and 4-dpmane fragments provides the estimate of polarization effect. It is noteworthy that all the complexes are structurally analogous. Hence, their electronic properties are also similar.

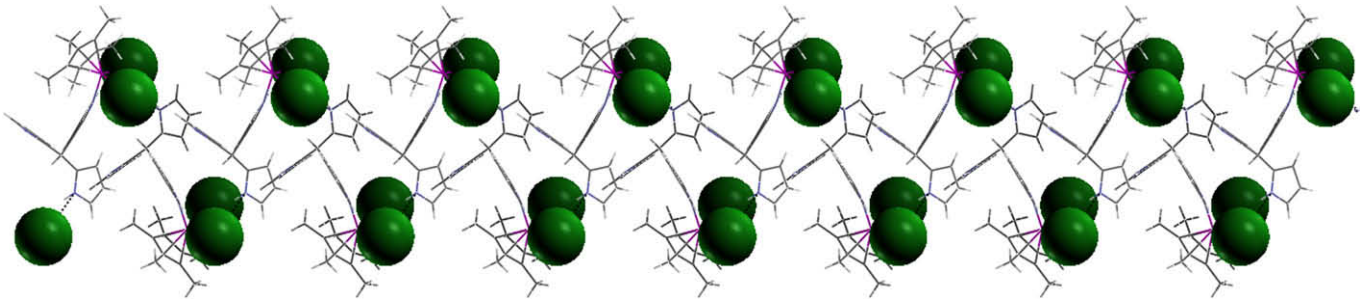

Fig. 5. Hydrogen bonding interaction leading to a zig-zag motif along crystallographic-'*a*' axis in complex **8**.

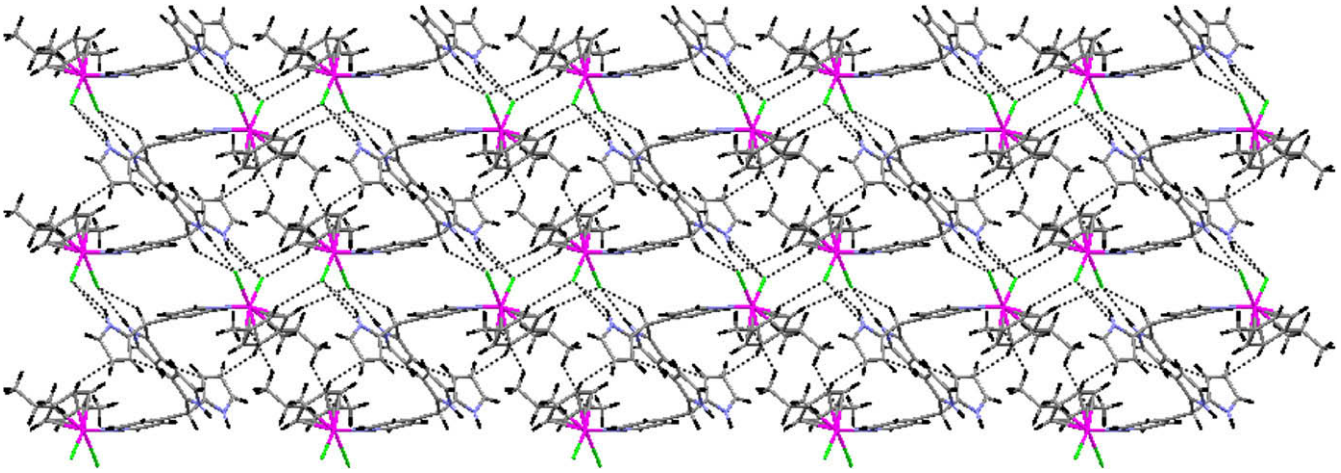

Fig. 6. Sheet like motif resulting from C–H···Cl and C–H···π weak interactions along crystallographic-'c' axis in complex **3**.

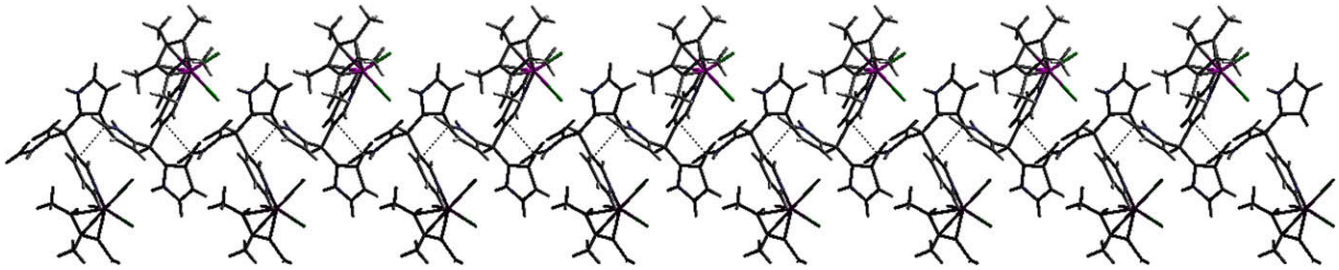

Fig. 7. Zig-zag motif resulting from π···π weak interactions along crystallographic-'c' axis in complex **8**.

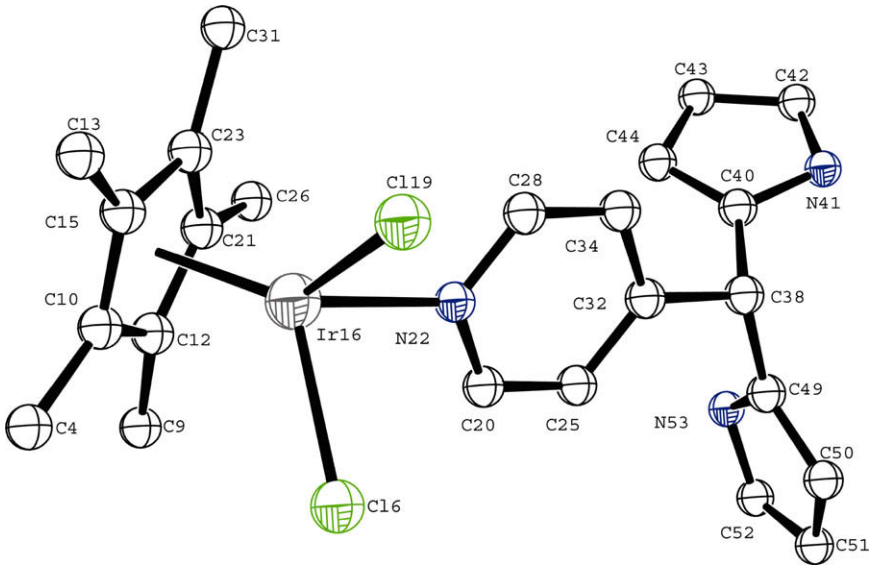

Fig. 8. Optimized geometries of **7** (ORTEP view at 30% probability, H atoms excluded for clarity).

3.4. Catalytic transfer hydrogenation of aldehyde

Based on the pioneering studies of many workers on transfer hydrogenation catalysis using half-sandwich organometallic Ru/Rh/Ir complexes, [63] and on our own efforts in this direction [37] we became interested to examine catalytic activity of the complexes under study towards reduction of the formyl group of aldehyde. Representative ruthenium complex **4**, rhodium complex **6** and iridium complex **8** were used as catalyst and terephthaldehyde, 4-nitrobenzaldeyde and 4-cyanobenzaldeyde as substrates. To compare the results we have taken analogous complexes $[(\eta^6\text{-}C_{10}H_{14})RuCl_2(4\text{-}CNPy)]$, $[(\eta^5\text{-}C_{10}H_{15})RhCl_2(4\text{-}CNPy)]$, $[(\eta^5\text{-}C_{10}H_{15})IrCl_2(4\text{-}CNPy)]$ imparting less bulkier 4-cyanopyridine, results shows only a small increase in yield. Respective reactions were initiated by introducing sodium formate and aldehydes (1.0 mmol) in water (trace of acetonitrile was used to dissolve the catalyst) under aerobic conditions at 80 °C using 2 mol% of the catalyst. Resulting data (Table 3) suggested that all the com-

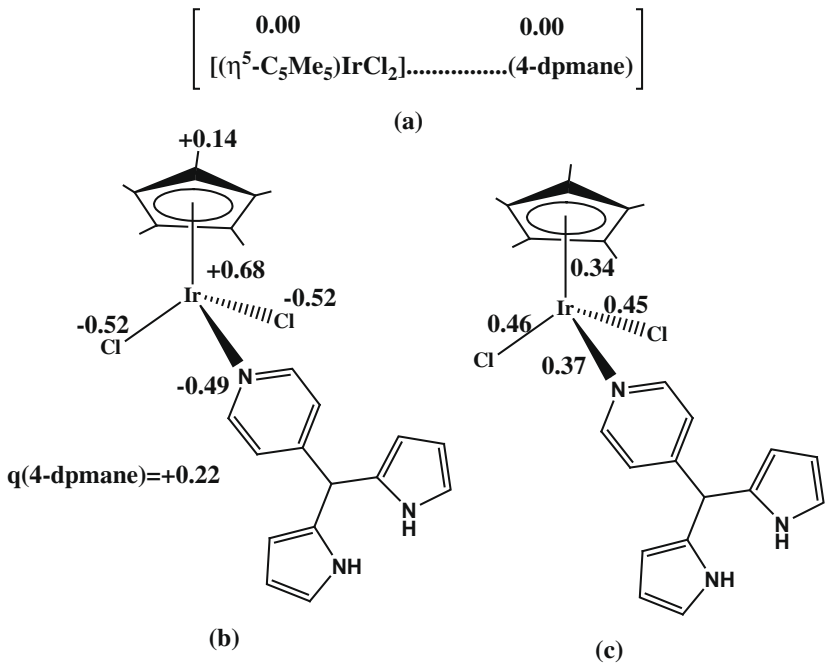

Scheme 3. (a) Charge distribution in different fragment when there is no bonding, (b) natural charge distribution on various groups, (c) Wiberg bond indices of bonds around metal centre.

Table 3
Transfer hydrogenation of aldehydes by [(η$^{6/5}$-C_xH_y)MCl_2(3-dpmane)].

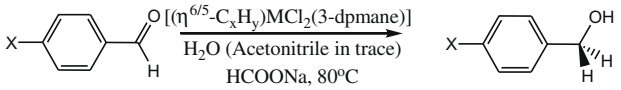

X = CHO, NO_2, CN

Catalyst	Aldehyde	% Con	*t*/h	TOF[a](h^{-1})
[(η^6-$C_{10}H_{14}$)$RuCl_2$(4-CNPy)]	Terephthaldehyde	80	10	4.0
[(η^5-C_5Me_5)$RhCl_2$(4-CNPy)]	Terephthaldehyde	89	5	8.9
[(η^5-C_5Me_5)$IrCl_2$(4-CNPy)]	Terephthaldehyde	85	7	6.0
[(η^6-$C_{10}H_{14}$)$RuCl_2$(3-dpmane)] (**4**)	Terephthaldehyde	74	10	3.7
[(η^5-C_5Me_5)$RhCl_2$(3-dpmane)] (**6**)	Terephthaldehyde	89	5	8.9
[(η^5-C_5Me_5)$IrCl_2$(3-dpmane)] (**8**)	Terephthaldehyde	80	7	5.7
[(η^6-$C_{10}H_{14}$)$RuCl_2$(4-CNPy)]	4-Nitrobenzaldeyde	85	10	4.2
[(η^5-C_5Me_5)$RhCl_2$(4-CNPy)]	4-Nitrobenzaldeyde	92	5	9.2
[(η^5-C_5Me_5)$IrCl_2$(4-CNPy)]	4-Nitrobenzaldeyde	86	5	8.6
[(η^6-$C_{10}H_{14}$)$RuCl_2$(3-dpmane)] (**4**)	4-Nitrobenzaldeyde	82	10	4.1
[(η^5-C_5Me_5)$RhCl_2$(3-dpmane)] (**6**)	4-Nitrobenzaldeyde	90	5	9
[(η^5-C_5Me_5)$IrCl_2$(3-dpmane)] (**8**)	4-Nitrobenzaldeyde	85	6	7.1
[(η^6-$C_{10}H_{14}$)$RuCl_2$(4-CNPy)]	4-Cyanobenzaldehyde	80	10	4.0
[(η^5-C_5Me_5)$RhCl_2$(4-CNPy)]	4-Cyanobenzaldehyde	90	5	9.0
[(η^5-C_5Me_5)$IrCl_2$(4-CNPy)]	4-Cyanobenzaldehyde	88	5	8.8
[(η^6-$C_{10}H_{14}$)$RuCl_2$(3-dpmane)] (**4**)	4-Cyanobenzaldehyde	80	10	4.0
[(η^5-C_5Me_5)$RhCl_2$(3-dpmane)] (**6**)	4-Cyanobenzaldehyde	87	5	8.7
[(η^5-C_5Me_5)$IrCl_2$(3-dpmane)] (**8**)	4-Cyanobenzaldehyde	87	5	8.7

[a] Based on% conversion; 4-CNPy = 4-cyanopyridine.

plexes are reasonably good hydrogen-transfer catalysts under aqueous and aerobic conditions. It is observed that in all these cases the formyl group of aldehyde is selectively reduced without affecting the other substituents (–CN, $–NO_2$). Interestingly, these complexes selectively reduce one formyl group of terephthaldehyde to produce 4-hydroxymethy-benzaldehyde. Further, it was observable that the rhodium and iridium complexes **6** and **8** are more effective in this regard than the ruthenium complex **4**. Resulting alcohols have been characterised by IR and ^{1}H NMR spectroscopy, and percentage conversions calculated by integration of the peaks in the NMR spectra.

4. Conclusions

In this work we have described synthesis, spectral and structural characterization of a series of neutral mononuclear complexes containing (η^6-arene)Ru-, (η^5-C_5Me_5)Rh- and (η^5-C_5Me_5)Ir-moieties and dipyrromethane ligands. Geometry and electronic structures of **7** have been optimized by theoretical studies and compared with the single crystal X-ray data of **8**. To determine bonding situation NBO calculations have also performed which suggested an overall charge flow in the direction M ← L. In addition, it has been shown that **4**, **6** and **8** acts as transfer hydro-

genation catalyst in the reduction of terephthaldehyde, 4-cyanobenzaldehyde and 4-nitrobenzaldehyde.

Acknowledgment

Thanks are due to the Council of Scientific and Industrial Research, New Delhi, India for providing financial assistance through the scheme [HRDG scheme no. 01(2074)/06/EMR-II]. We are also thankful to the Head, Department of Chemistry, Banaras Hindu University, Varanasi (U.P.) India and Prof. P. Mathur, Indian Institute of Technology, Powai, Mumbai, for providing single crystal X-ray data.

Appendix A. Supplementary material

CCDC 752429 and 752430 contain the supplementary crystallographic data for compounds **3** and **8**. These data can be obtained free of charge from The Cambridge Crystallographic Data Centre via www.ccdc.cam.ac.uk/data_request/cif.

Supplementary data associated with this article can be found, in the online version, at doi:10.1016/j.jorganchem.2010.01.006.

References

[1] J.S. Lindsey, Acc. Chem. Res. (2009), doi: 10.1021/ar900212t.
[2] S. Shanmugathasan, C. Edwards, R.W. Boyle, Tetrahedron 56 (2000) 1025–1046.
[3] C.M. Drain, J.T. Hupp, K.S. Suslick, M.R. Wasielewski, X. Chen, J. Porphyrins Phthalocyanines 6 (2002) 243–258.
[4] I. Okura, J. Porphyrins Phthalocyanines 6 (2002) 268–270.
[5] R. Bonnett, Chem. Soc. Rev. 24 (1995) 19–33.
[6] E.D. Sternberg, D. Dolphin, C. Bruckner, Tetrahedron 54 (1998) 4151–4202.
[7] I.J. MacDonald, T.J. Dougherty, J. Porphyrins Phthalocyanines 5 (2001) 105–129.
[8] Porphyrins and Metalloporphyrins; K.M. Smith (Ed.), Synthesis and Preparation of Porphyrin Compounds, Elsevier, 1975 (Chapter 2).
[9] The Porphyrins; in: D. Dolphin (Ed.), Synthesis of Pyrroles and Porphyrins via Single Step Coupling of Dipyrrolic Intermediates. Academic Press, 1978 (Chapter 4).
[10] B.J. Littler, M.A. Miller, C.H. Hung, R.W. Wagner, D.F. O'Shea, P.D. Boyle, J.S. Lindsey, J. Org. Chem. 64 (1999) 1391–1396. and references therein.
[11] T.E. Wood, A. Thompson, Chem. Rev. 107 (2007) 1831. and reference therein; S.R. Halper, S.M. Cohen, Inorg. Chem. 44 (2005) 486–488.
[12] D.L. Murphy, M.R. Malachowski, C.F. Campana, S.M. Cohen, A chiral, Chem. Commun. (2005) 5506–5508.
[13] H. Maeda, M. Hasegawa, T. Hashimoto, T. Kakimoto, S. Nishio, T. Nakanishi, J. Am. Chem. Soc. 128 (2006) 10024–10025.
[14] S.J. Garibay, J.R. Stork, Z. Wang, S.M. Cohen, S.G. Telfer, Chem. Commun. (2007) 4881–4883.
[15] E. Barnea, A.L. Odom, Dalton Trans. (2008) 4050–4054.
[16] Y. Shi, C. Hall, J.T. Ciszewski, C. Cao, A.L. Odom, Chem. Commun. (2003) 586–587.
[17] D.L. Swartz II, Aaron L. Odom, Dalton Trans. 107 (2008) 4254–4258.
[18] I. Vidyaratne, P. Crewdson, E. Lefebvre, S. Gambarotta, Inorg. Chem. 46 (2007) 8836–8842.
[19] E.A. Katayev, Y.A. Ustynyuk, V.M. Lynch, J.L. Sessler, Chem. Commun. (2006) 4682–4684.
[20] E.A. Katayev, K. Severin, R. Scopelliti, Y.A. Ustynyuk, Inorg. Chem. 46 (2007) 5465–5467.
[21] W. Chung Chen, C.P. Lau, S. Cheng, V.S. Leung, J. Organomet. Chem. 464 (1994) 103–106.
[22] B. Seiller, C. Brulleu, P.H. Dexneuf, J. Chem. Soc., Chem. Commun. (1994) 493–494.
[23] M.A. Bennett, M.I. Bruce, T.W. Matheson, in: G. Wilkinson, F.G.A. Stone, E.W. Abel (Eds.), Comprehensive Organometallic Chemistry, vol. 4, Pergamon, Oxford, 1982, p. 796.
[24] R.H. Crabtree, The Organometallic Chemistry of the Transition Metals, John Wiley and Sons, Hoboken, NJ, 2005.
[25] For highlights of important developments in the metal–ligand cooperative activation of substrates, see: H. Grützmacher, Cooperating Ligands in Catalysis, Angew. Chem., Int. Ed. 47 (2008) 1814–1818.
[26] J. Liu, X. Wu, J.A. Iggo, J. Xiao, Coord. Chem. Rev. 252 (2008) 782–809.
[27] K. Severin, Chem. Commun. 31 (2006) 3859–3867.
[28] D.H. Dresnah, M.C. Baird, J. Organomet. Chem. 127 (1977) C55–C58. and references therein.
[29] M. Auzias, J. Gueniat, B. Therrien, G. Süss-Fink, A.K. Renfrew, P.J. Dyson, J. Organomet. Chem. 694 (2009) 855–861.
[30] H. Brunner, R.C. Gastinger, J. Organomet. Chem. 145 (1978) 365–373.
[31] W.F. Sheldrick, S. Heeb, J. Organomet. Chem. 377 (1989) 357–366.
[32] W.F. Sheldrick, S. Heeb, Inorg. Chim. Acta 168 (1990) 93–100.
[33] R. Kramer, M. Maurus, R. Bergs, K. Polborn, K. Sunkel, B. Wagner, W. Beck, Chem. Ber. 126 (1993) 1969–1980. and references therein.
[34] S.K. Mandal, A.R. Chakravarty, Inorg. Chem. 32 (1993) 3851–3854. and references therein.
[35] H. Brunner, R. Oeschey, B. Nuber, Inorg. Chem. 34 (1995) 3349–3351.
[36] G. Capper, L.C. Carter, D.L. Davies, J. Fawcett, D.R. Russel, J. Chem. Soc., Dalton Trans. (1996) 1399–1403.
[37] M. Yadav, A.K. Singh, D.S. Pandey, Organometallics 28 (2009) 4713–4723.
[38] M. Yadav, A.K. Singh, B. Maiti, D.S. Pandey, Inorg. Chem. 48 (2009) 7593–7603.
[39] M. Yadav, P. Kumar, A.K. Singh, J. Ribos, D.S. Pandey, Dalton Trans. (2009) 9929–9934.
[40] M. Yadav, P. Kumar, D.S. Pandey, Polyhedron (2009), doi:10.1016/j.poly.2009.10.028.
[41] D.D. Perrin, W.L.F. Armango, D.R. Perrin, Purification of Laboratory Chemicals, Pergamon, Oxford, UK, 1986.
[42] D. Gryko, J.S. Lindsey, J. Org. Chem. 65 (2000) 2249–2252.
[43] M.A. Bennett, T.N. Huang, T.W. Matheson, A.K. Smith, Inorg. Synth. 21 (1982) 74–78.
[44] M.A. Bennett, A.K. Smith, J. Chem. Soc., Dalton Trans. (1974) 233–241.
[45] W. Kang, K. Moseley, P.M. Maitlis, J. Am. Chem. Soc. 91 (1969) 5970–5977.
[46] C. White, A. Yates, P.M. Maitilis, Inorg. Synth. 29 (1992) 228–234.
[47] G.M. Sheldrick, SHELX-97: Programme for Refinement of Crystal Structures, University of Göttingen, Göttingen, Germany, 1997.
[48] A.D. Becke, J. Chem. Phys. 98 (1993) 5648–5652.
[49] C.T. Lee, W.T. Yang, R.G. Parr, Phys. Rev. B 37 (1988) 785–789.
[50] R. Krishnan, J.S. Binkley, R. Seeger, J.A. Pople, J. Chem. Phys. 72 (1980) 650–654.
[51] A.D. McClean, G.S. Chandler, J. Chem. Phys. 72 (1980) 5639–5648.
[52] P. Hay, W.R. Wadt, J. Chem. Phys. 82 (1985) 270–283.
[53] W.R. Wadt, P. Hay, J. Chem. Phys. 82 (1985) 284–298.
[54] P. Hay, W.R. Wadt, J. Chem. Phys. 82 (1985) 299–310.
[55] W. Kohn, L.J. Sham, Phys. Rev. 140 (1965) A1133–A1138.
[56] M.J. Frisch, G.W. Trucks, H.B. Schlegel, G.E. Scuseria, M.A. Robb, J.R. Cheeseman, J.A. Montgomery, Jr., T. Vreven, K.N. Kudin, J.C. Burant, J.M.Millam, S.S. Iyengar, J. Tomasi, V. Barone, B. Mennucci, M. Cossi, G. Scalmani, N. Rega, G.A. Petersson, H. Nakatsuji, M. Hada, M. Ehara, K. Toyota, R. Fukuda, J. Hasegawa, M. Ishida, T. Nakajima, Y. Honda, O. Kitao, H. Nakai, M. Klene, X. Li, J.E. Knox, H.P. Hratchian, J.B. Cross, V. Bakken, C. Adamo, J. Jaramillo, R. Gomperts, R.E. Stratmann, O. Yazyev, A.J. Austin, R. Cammi, C. Pomelli, J. Ochterski, P.Y. Ayala, K. Morokuma, G.A. Voth, P. Salvador, J.J. Dannenberg, V.G. Zakrzewski, S. Dapprich, A.D. Daniels, M.C. Strain, O. Farkas, D.K. Malick, A.D. Rabuck, K. Raghavachari, J.B. Foresman, J.V. Ortiz, Q. Cui, A.G. Baboul, S. Clifford, J. Cioslowski, B.B. Stefanov, G. Liu, A. Liashenko, P. Piskorz, I. Komaromi, R.L.Martin, D.J. Fox, T. Keith, M.A. Al-Laham, C.Y. Peng, A. Nanayakkara, M. Challacombe, P.M.W. Gill, B.G. Johnson, W. Chen, M.W. Wong, C. Gonzalez, J.A. Pople, GAUSSIAN 03 (Revision D.01), Gaussian, Inc., Wallingford, CT, 2004.
[57] A. Singh, N. Singh, D.S. Pandey, J. Organomet. Chem. 642 (2002) 48–57.
[58] A. Singh, A.N. Sahay, D.S. Pandey, M.C. Puerta, P. Valerga, J. Organomet. Chem. 605 (2000) 74–81.
[59] S.K. Singh, M. Trivedi, M. Chandra, A.N. Sahay, Inorg. Chem. 43 (2004) 8600–8608. and references cited therein.
[60] P. Govindaswamy, Y.A. Mozharivskyj, M.K. Rao, Polyhedron 26 (2007) 5039–5044.
[61] P. Govindaswamy, Y.A. Mozharivskyj, Polyhedron 24 (2005) 1710–1716.
[62] K.T. Prasad, G. Gupta, A.V. Rao, B. Das, M.K. Rao, Polyhedron 28 (2009) 2649–2654.
[63] X. Wu, J. Xiao, Chem. Commun. 46 (2007) 2449–2466. and reference therein.